

See discussions, stats, and author profiles for this publication at: <https://www.researchgate.net/publication/272390839>

Assembly of Ferrocene Molecules on Metal Surfaces Revisited

ARTICLE *in* JOURNAL OF PHYSICAL CHEMISTRY LETTERS · FEBRUARY 2015

Impact Factor: 7.46 · DOI: 10.1021/jz5026118

CITATIONS

2

READS

48

9 AUTHORS, INCLUDING:



[Roberto Robles](#)

Catalan Institute of Nanoscience and Nanotec...

61 PUBLICATIONS 592 CITATIONS

[SEE PROFILE](#)



[Martin Vérot](#)

Ecole normale supérieure de Lyon

6 PUBLICATIONS 50 CITATIONS

[SEE PROFILE](#)



[Tangui Le Bahers](#)

Claude Bernard University Lyon 1

33 PUBLICATIONS 856 CITATIONS

[SEE PROFILE](#)



[Nicolás Lorente](#)

Spanish National Research Council

144 PUBLICATIONS 3,280 CITATIONS

[SEE PROFILE](#)

Assembly of Ferrocene Molecules on Metal Surfaces Revisited

Maider Ormaza,^{*,†} Paula Abufager,^{‡,§} Nicolas Bachellier,[†] Roberto Robles,^{‡,||} Martin Verot,[⊥] Tangui Le Bahers,[⊥] Marie-Laure Bocquet,[⊥] Nicolas Lorente,^{‡,||} and Laurent Limot[†]

[†]Institut de Physique et Chimie des Matériaux de Strasbourg, Université de Strasbourg, UMR CNRS 7504, 67034 Strasbourg, France

[‡]ICN2—Institut Català de Nanociència i Nanotecnologia, Campus UAB, 08193 Bellaterra, Barcelona, Spain

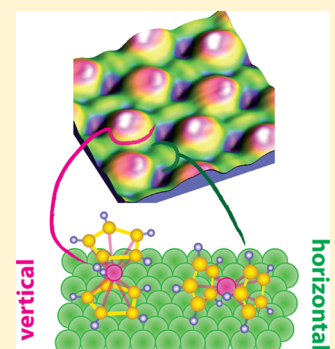
[§]Instituto de Física de Rosario, Consejo Nacional de Investigaciones Científicas y Técnicas (CONICET) and Universidad Nacional de Rosario, Av. Pellegrini 250, 2000 Rosario, Argentina

^{||}CSIC -Consejo Superior de Investigaciones Científicas, ICN2 Building, Campus UAB, 08193 Bellaterra, Barcelona, Spain

[⊥]Université de Lyon, Université Claude Bernard Lyon 1, Centre National de Recherche Scientifique, ENS Lyon, 46 allée d'Italie, 69007 Lyon Cedex 07, France

 Supporting Information

ABSTRACT: Metallocene (MCP_2) wires have recently attracted considerable interest in relation to molecular spintronics due to predictions concerning their half-metallic nature. This exciting prospect is however hampered by the little and often-contradictory knowledge we have concerning the metallocene self-assembly and interaction with a metal. Here, we elucidate these aspects by focusing on the adsorption of ferrocene on Cu(111) and Cu(100). Combining low-temperature scanning tunneling microscopy and density functional theory calculations, we demonstrate that the two-dimensional molecular arrangement consists of vertical- and horizontal-lying molecules. The noncovalent T-shaped interactions between Cp rings of vertical and horizontal molecules are essential for the stability of the physisorbed molecular layer. These results provide a fresh insight into ferrocene adsorption on surfaces and may serve as an archetypal reference for future work with this important variety of organometallic molecules.



Metallocenes were discovered in the fifties and have boosted the development of organometallic chemistry, in part earning Fischer and Wilkinson the Nobel Prize in chemistry in 1973. Metallocenes are organometallic sandwich compounds of simplified architecture as built on two cyclopentadienyl rings ($C_5H_5^-$, Cp) bound through a metal center, for example, by Fe^{2+} in the case of ferrocene (see Figure 1). In the past decade, metallocenes were again in the spotlight in relation to molecular spintronics. This emerging technology exploits the spin to convey information in hybrid metal–

molecule devices.¹ These molecules are extremely appealing as they ensure high device efficiency and offer the unique possibility of having built-in spin functionalities. Numerous theoretical investigations have demonstrated that metallocene wires can in fact produce a nearly ideal spin-polarized current, in other words, a current with 100% spin polarization.^{2–8} Despite this exciting prospect, the design of devices incorporating metallocenes has been held up by the limited knowledge we have concerning their interaction with a metal. After all, the device performance will be dictated by the adsorption geometry, molecular self-assembly, and spin-state at a metal surface.⁹

There is little consensus on the way these molecules adsorb onto surfaces. Several studies have reported an associative adsorption at low temperature of ferrocene ($FeCp_2$) on $Ag^{10–12}$, Cu^{11} , graphite,^{13,14} and Mo^{15} by means of photo-emission (PES) and electron energy loss spectroscopy (EELS), claiming a preferential orientation of the molecular axis perpendicular or parallel to the surface depending on the substrate (Figure 1a). On the other hand, based on STM measurements, K. F. Braun et al.¹⁶ proposed a dissociative adsorption model of $FeCp_2$ on $Au(111)$, whereas an associative adsorption has been addressed for various ferrocene-derived

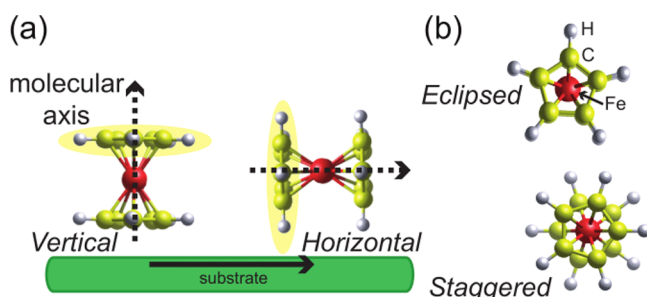


Figure 1. (a) Different positions, vertical and horizontal, of a ferrocene with respect to the surface. The molecular axis in both cases is indicated with a dashed arrow. White, yellow, and red balls represent H, C, and Fe atoms, respectively. (b) Eclipsed and staggered conformations of a ferrocene molecule.

Received: December 10, 2014

Accepted: January 12, 2015

Published: January 12, 2015

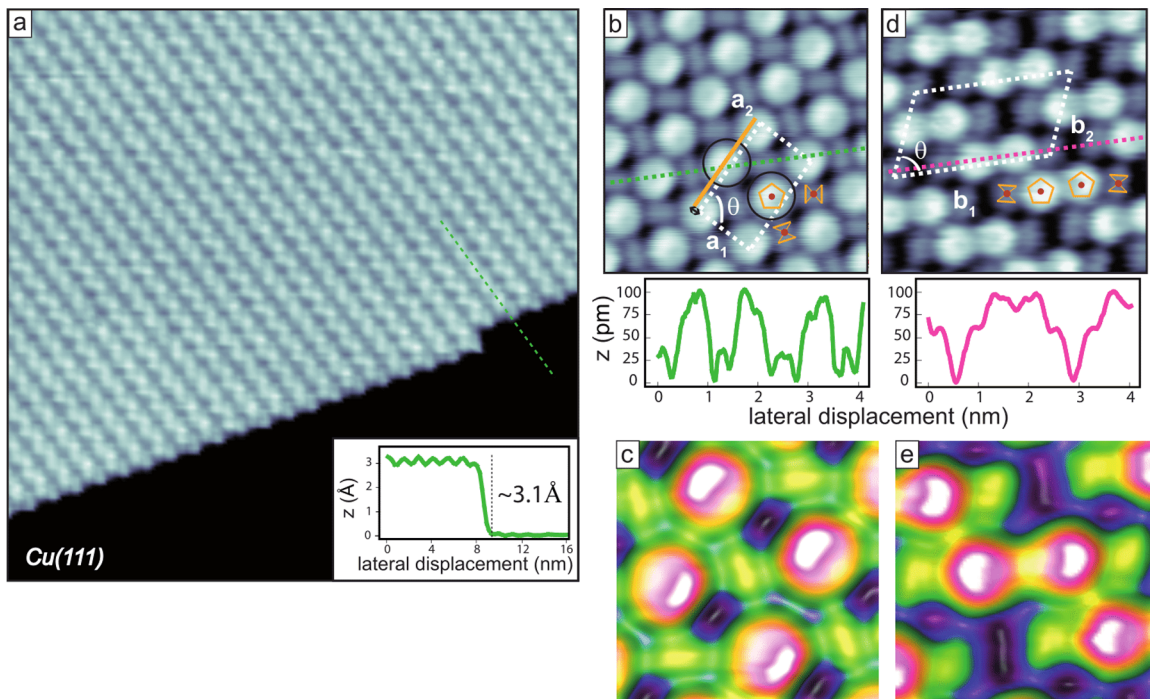


Figure 2. (a) STM image of 0.6 monolayer FeCp_2 deposited on $\text{Cu}(111)$ (+1 V, 0.5 nA). Inset: Height profile of the molecular monolayer. Two different configurations are observed on $\text{Cu}(111)$: (b) compact (-1 V, 0.5 nA) and (d) zigzag (+0.1 V, 0.2 nA). The unit cells (white dashed lines), composed of vertical and horizontal molecules, as well as the line profiles of both arrangements, are shown in each image. (b–d) Close-up view of the two configurations, highlighting the asymmetry of the rings in the vertical molecules. Image sizes: (a) $30 \times 30 \text{ nm}^2$, (b–d) $4 \times 4 \text{ nm}^2$, (c–e) $2 \times 2 \text{ nm}^2$.

Table 1. Unit Cell Parameters^a and Energetics of Compact and Zigzag Arrangements^b

Compact	a_1 (Å)	a_2 (Å)	θ (deg)
Experiment	8.9 ± 0.3	15.5 ± 0.3	90 ± 3
Theory	8.75	15.15	90
E_{ads} (eV)	E_{ads}^{vdW} (eV)	E_{coh}^{free} (eV)	$q(e^-)$
1.35	1.05	0.48	$d(\text{\AA})$

Zigzag	b_1 (Å)	b_2 (Å)	θ (deg)
Experiment	23.0 ± 0.4	13.0 ± 0.4	71 ± 3
Theory	23.15	13.37	68
E_{ads} (eV)	E_{ads}^{vdW} (eV)	E_{coh}^{free} (eV)	$q(e^-)$
1.26	1.02	0.43	$d(\text{\AA})$

^a a_1 , a_2 , b_1 , b_2 , θ . ^b E_{ads} (adsorption energy per molecule), E_{ads}^{vdW} (van der Waals (vdW) contribution per molecule coming from the molecule–substrate interaction), E_{coh}^{free} (cohesive energy per molecule for the free-standing overlayer), q (molecule–substrate charge transfer per unit cell), $d_{\text{mol–surf}}$ (molecule–surface distance).

molecules on the same substrate.^{17,18} B. W. Heinrich and co-workers¹⁹ presented a molecularly physisorbed ferrocene on $\text{Cu}(111)$ lying with the molecular axis perpendicular to the surface.

The adsorption of metallocenes remains elusive up to now. In this work, we aim to clarify the self-assembly, adsorption geometry, and interactions of ferrocene molecules deposited on a metallic surface. By means of scanning tunneling microscopy (STM) and density functional theory (DFT), we show how associatively adsorbed FeCp_2 molecules self-assemble on a Cu surface adopting a configuration that is independent of the surface orientation, dismissing the idea of a unique preferential orientation of the molecular axis with respect to the substrate

suggested by previous works. In fact, the stability of the two-dimensional structure depends crucially on a combination of vertical (molecular axis perpendicular to the surface, Figure 1a) and horizontal (axis parallel to the surface) molecules having their Cp rings in a so-called eclipsed configuration (D_{sh} symmetry, Figure 1b). Interestingly, this arrangement bears similarities with both the gas phase and the bulk structure of ferrocene. Similar to the ferrocene crystal (see Figure 4e), the presence of the two molecules, vertical and horizontal, ensures the cohesion of the crystal through T-shaped interactions, but as in the gas phase—and unlike bulk ferrocene—the eclipsed configuration is favored over the staggered configuration (D_{sd} symmetry, Figure 1b).

The adsorption of FeCp_2 on a cold Cu(111) surface gives rise to long-range well-ordered molecular layers with almost no defects and exhibiting an apparent height of 3.1 Å (Figure 2a). Two different molecular configurations, which we label “compact” and “zigzag” (see Figure 2b and d, respectively), appear equally distributed across the surface. Identical results are observed for FeCp_2 deposited on Cu(100) (see Supporting Information).

In the compact configuration, elongated rod-like protrusions are observed in between ring-like protrusions. We assign these ring-like units to the Cp rings of vertical FeCp_2 , whereas the rod-like protrusions, showing a height 0.5 Å smaller, are assigned to horizontal FeCp_2 . The corrugation observed along the dashed green line in Figure 2b due to the presence of both, vertical and horizontal, molecules is shown in the line profile below the image. The rectangular unit cell of the compact configuration is marked in white. The cell, with lattice parameters a_1 , a_2 , and angle θ (see Table 1 for values), contains four molecules, two horizontal and two vertical. As shown, consecutive vertical molecules in the a_2 direction do not lie exactly in the same axis (see the orange axis and the molecules marked with circles in Figure 2b), they are shifted by 1.5 Å. Moreover, vertical molecules present an asymmetry in the a_1 direction, being brighter on one side of the ring; vertical molecules in the center and in the corner of the unit cell show the asymmetry at different sides of the ring. This asymmetry can be clearly observed in Figure 2c and, as we show later, indicates that the molecules are tilted.

Figure 2d presents the zigzag configuration in which two ring-like protrusions, corresponding to vertical molecules, form a dimer-like pair. They are flanked by horizontal molecules that have a dimmer contrast in the image. The line profile taken along the pink dashed line shows the corrugation of the molecular assembly. Similarly to the compact case, the apparent height difference between vertical and horizontal molecules is around 0.5 Å. The distance between the two adjacent dimer-like vertical molecules is (6.2 ± 0.2) Å, which is small compared to the (8.0 ± 0.2) Å found for the compact arrangement. The unit cell is a parallelogram (see parameters in Table 1), as shown in white in Figure 2d. A similar ferrocene pairing has been also observed for ferrocene-derived molecules (FeCp_2COOH and $\text{FeCp}_2(\text{CH}_2)_n\text{-FeCp}_2$) deposited on metallic surfaces.^{18,20}

Although the identification of vertical ferrocene molecules is straightforward, determining the presence of the horizontal molecules is experimentally challenging. Therefore, to confirm the proposed adsorption model for ferrocene, we rotated some molecules from a vertical (horizontal) to a horizontal (vertical) position by using the STM tip,²¹ as shown in the before-and-after images in Figure 3. The molecular structure of FeCp_2 is superimposed in the images below (the structure used has an arbitrary orientation). Upon application of a bias pulse of 2 V, molecules rotate out-of-plane from horizontal to vertical (molecules noted 1 and 2), or vice versa (molecules noted 3 and 4). There are likely in-plane rotations more difficult to identify. Clearly, when the vertical axis of FeCp_2 is rotated nearly 90° parallel to the surface, the ring-like feature is lost, confirming the presence of both vertical and horizontal molecules on the surface.

In order to study the stability and electronic properties of the structures proposed for the molecular layer on Cu(111), we have performed extensive DFT calculations and simulated the corresponding STM images. First, we started by studying the

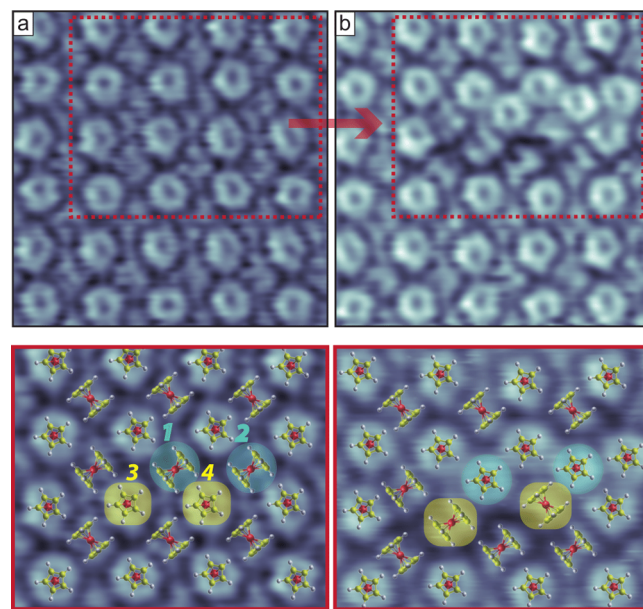


Figure 3. STM images (+1 V, 1 nA) of the compact configuration on Cu(111) before and after some molecules turned from a vertical to a horizontal position, or vice versa, via tip-assisted manipulation. The images below correspond to the marked squares in the pictures above, with the molecules superimposed to highlight the molecules that have rotated (1–4). Notice that a molecular tip has been employed in order to enhance the observed features. Additionally, a Laplacian filter has been applied. Image sizes: (a-b) 4.5×4.5 nm².

intramolecular structure of ferrocene molecules. As shown in Figure 1b, two different configurations can be found for a ferrocene molecule: eclipsed and staggered. The former one corresponds to the most stable structure in the gas phase,^{22–24} whereas the latter is the most common one in the solid state.²⁵ We found that the eclipsed configuration is more stable by 45 meV on the surface. According to our calculations, no matter what initial configuration is chosen, the eclipsed structure is always preferred for both horizontal and vertical molecules. In the molecular layer discussed hereafter, we find exclusively molecules in the eclipsed configuration.

We focused then on the intermolecular arrangement of both compact and zigzag configurations. Let us first concentrate on the analysis of the compact configuration. In Figure 4a and b, different views of the most stable calculated structure, together with a simulated STM image, are shown. The rectangular unit cell observed in the STM images (Figure 2b) corresponds within experimental accuracy to a $2 \times 6\sqrt{3}$ unit cell in the Cu(111) surface (see Table 1). The stability of the proposed structure has been tested using this unit cell.

Comparing the simulated STM image (Figure 4a) with the experimental one (Figure 2b), we observe that the main features of the image are reproduced. The structure shown in Figure 4b, in which the minimum distance from the surface to the molecule is 2.3 Å, allows us to explain all these signatures. Rod-like and ring-like protrusions in the image correspond to horizontal and vertical molecules, respectively. A strong contrast difference is observed between both molecules in the STM images. At first glance, this contrast appears counter-intuitive as horizontal molecules appear dimmer, despite that some of their H atoms are 0.2 Å further away into vacuum compared to the Cp ring of the vertical molecules (side view of Figure 4b). This apparent contradiction can be easily lifted by

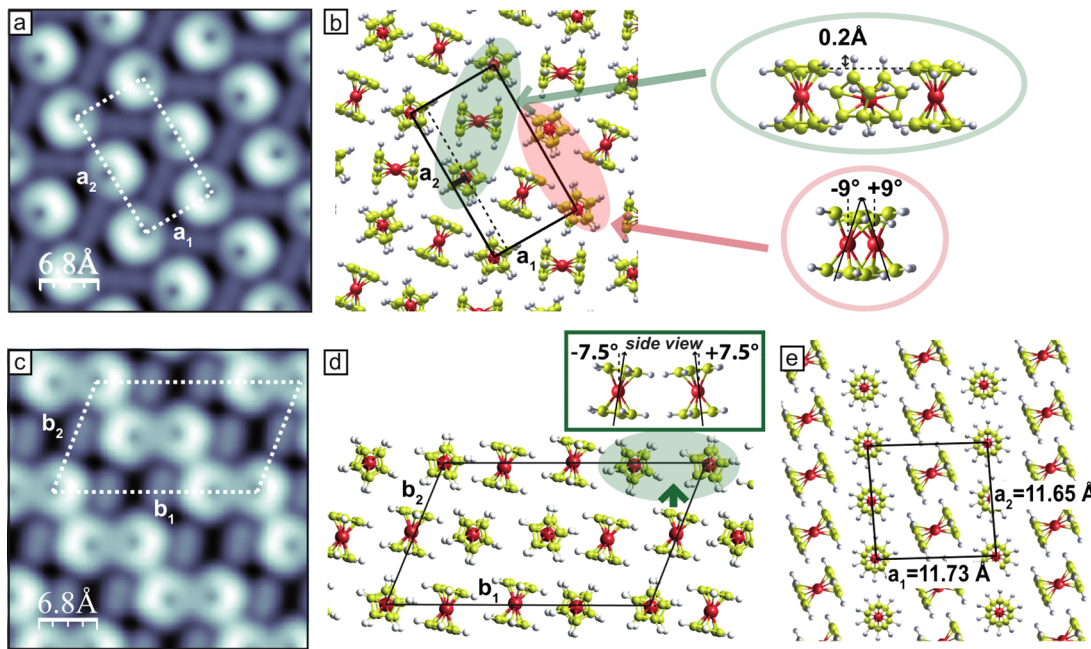


Figure 4. (a–c) Simulated STM topographic images for a bias of 1 V corresponding to the relaxed (b) compact and (d) zigzag structures on the Cu(111) surface. Lateral views of the indicated molecules are shown in both cases in order to present the relative position and tilt between molecules. (e) Crystallographic (100) plane of the bulk solid ferrocene.

recalling that the tunneling transmission probability between the STM tip and the molecule depends on the tip and molecular orbitals. Orbitals that extend into the vacuum, such as s , p_z or d_z^2 , will be favored in the tunneling process. In the present case, for vertical molecules, the d-manifold orbital of Fe lies around the Fermi level and hybridizes with the p orbitals perpendicular to the Cp rings that protrude into the vacuum, enhancing the coupling with the tip orbitals. In contrast, for horizontal molecules, the p orbitals of the organic ring lie in a plane parallel to the surface and do not point toward the STM tip. Hence, the simulated apparent height of the vertical molecules is 0.5 Å higher, in agreement with the experimentally measured line profiles shown in Figure 2b.

Our calculations also reproduce subtle effects revealed by STM images. We observe a lateral displacement of 1.49 Å between consecutive vertical molecules in the a_2 direction (marked in Figure 4b), measured as the distance between Fe atoms, which is consistent with the experimentally found shift of 1.5 Å (marked in Figure 2b). Most importantly, we find that the slight asymmetry observed for the ring of the vertical molecules (Figure 2c) results from a tilt between successive vertical molecules in the a_2 direction. This is a robust feature of the molecular layer, as in our computation, an initial configuration with no tilt always relaxes until a tilt is present. The origin of the tilt lies in the presence of the horizontal molecules. In particular, we found that the most stable situation is the one in which the horizontal molecules have two H atoms of each Cp ring pointing toward the surface; in this case, this leaves a single H atom per Cp ring pointing into the vacuum. This configuration gives rise to a 18° tilt between vertical molecules, as shown in the lateral view in Figure 4b.

In order to understand the intermolecular interactions, the nature of the interaction between two type of FeCp₂ molecules was investigated. We found that the adsorption energy per molecule is 1.35 eV, where the contribution from the van der Waals (vdW) dispersion forces amounts to 1.05 eV (see

Theoretical Methods). Comparing the difference between both numbers (0.30 eV) to the cohesion energy of the free-standing monolayer (0.48 eV), it can be concluded that the interaction between the molecules and the surface is due to vdW forces. The modest charge transfer per unit cell from the substrate to the molecules (0.11 e⁻) points to molecules being physisorbed on the surface. This conclusion is supported by the fact that the presence of the surface is not necessary to stabilize the molecular layer. Calculations of the unsupported monolayer show that the free-standing structure is stable, and it presents the main features of the supported situation, including the tilt of the vertical molecules. Moreover, when the layer is moved to different positions with respect to the copper surface (top, bridge, hcp, fcc), the energy cost is only of the order of 0.1 eV per unit cell. Additionally, experimental results indicating that the same molecular assembly is observed independently of the copper surface symmetry reinforce the idea of molecular physisorption (see Supporting Information).

As shown in Figure 4e, the (100) plane of pure ferrocene bulk (monoclinic phase P21/a) exhibits a very similar arrangement to the compact structure observed on the surface. This confirms that the alternative orientation of a ferrocene network is frequently encountered even outside surface science. However, it can be noticed that in the primitive cell observed and computed for the compact structure (Figure 4b), adjacent eclipsed horizontal molecules are oriented differently, contrary to the unit cell of staggered ferrocenes shown by the bulk in Figure 4e. As in the crystalline structure, in this case we have also seen how the cohesion of the layer mainly comes from vdW interactions.

To conclude, we consider now the zigzag structure. Due to the size of the parallelogram unit cell (see parameters in Table 1), we have just performed a few calculations to confirm the stability of the proposed structure. Figure 4c shows the simulated topographic STM image corresponding to the most stable structure that has been found (Figure 4d), which

reproduces with high accuracy the main features of the experimental image (Figure 2d). This structure shares some common features with the compact structure. First, the same reversal of the apparent height is observed, in which horizontal molecules always appear dimmer in the images, although the highest atom of horizontal molecules in this case is placed 0.4 Å further from the surface than the topmost atom of the vertical ones. Second, we also find that four H atoms of the horizontal molecules have to point toward the surface in order to get a stable structure. Third, a 15° tilt in two opposite directions is also observed for the vertical molecules (side view of Figure 4d), explaining the experimentally observed asymmetry between vertical molecules shown in Figure 2e.

According to an analysis of the energetics of the zigzag configuration, the adsorption energy per molecule is 1.26 eV, of which 1.02 eV comes from the contribution of vdW forces. The interaction between the molecules and the copper surface is mainly related to vdW forces, as may be concluded after comparing these adsorption values with the cohesion energy of the free-standing monolayer (0.43 eV). There is a moderate charge transfer per unit cell, 0.18 e⁻, which is also indicating a weak molecule–substrate interaction. Table 1 summarizes the energetics of the adsorption of both, compact and zigzag, configurations, showing that they are very similar, pointing in both cases to the same conclusion of a physisorbed layer.

We have presented a complete experimental and theoretical study of ferrocene molecules adsorbed onto copper surfaces, which solves the long-standing dilemma concerning the self-assembly of ferrocene on a metal surface. We demonstrate that ferrocene molecules adsorb associatively, forming two different self-assemblies, compact and zigzag, which appear equally distributed on the surface. These arrangements, which include the presence of vertical and horizontal molecules, are lead by intermolecular interactions, in particular T-shaped interactions, which are essential to stabilize the structures and to explain subtle submolecular features resolved in the STM images. As in the gas-phase ferrocene, the eclipsed configuration is found to be the most stable one for molecules adsorbed on a copper surface, whereas the presence of vertical and horizontal molecules on the surface is reminiscent of the crystallographic structure of bulk ferrocene. The fact that the same configurations, compact and zigzag, are found in differently oriented copper surfaces, together with the small charge transfer and the vdW interaction between the molecular monolayer and the Cu surface, confirms the physisorption of the molecules. We believe that these results may provide a solid guideline for future investigations on ferrocene, and eventually, related metallocenes on surfaces.

Experimental Methods. Samples have been prepared in a ultrahigh vacuum (UHV) chamber at a base pressure of 10⁻¹⁰ mbar equipped with a LT-STM operating at 4.5 K. The Cu(111) and Cu(100) metallic surfaces were cleaned by repeated Ar⁺ ion bombardments and annealing treatments at 860 K until clean large terraces were obtained. FeCp₂ molecules were sublimated at room-temperature in vacuo on the metallic cold surfaces (\leq 100 K) with a deposition rate of approximately 1.2 mL/min. After the molecular deposition, the samples were immediately cooled to 4.5 K for STM measurements. In situ cleaned W tips were used for measurements. WSxM software has been used for data analysis.²⁶

Theoretical Methods. We have studied the geometric and electronic structures of the adsorbed molecules by performing ab initio density functional theory calculations as implemented

in the VASP code.²⁷ We have used a plane wave basis set to expand the wave functions with a cutoff energy of 400 eV. Core electrons have been treated using the projector augmented wave method,^{28,29} and we have used the generalized gradient approximation in the PBE form for the exchange and correlation functional.³⁰ The long-range dispersion corrections have been treated using the DFT+D2 approach proposed by Grimme.³¹ Although this empirical vdW correction remains an approximation, it readily corrects the major lack of GGA energies and enables a qualitative description of the interactions at play in the self-assembly process. The interaction energies computed with this approach allow only to highlight the role of the dispersion interaction in the auto-organization process. Charge transfer has been obtained by performing a Bader analysis.³²

The Cu(111) surface has been modeled using a slab geometry with five Cu layers and a vacuum region of 19 Å. We have kept fixed the bottom three Cu layers, allowing the two topmost layers and the ferrocene atoms to relax until forces were smaller than 0.02 eV/Å. The D2 lattice constant of Cu has been used (3.572 Å). The compact structure has been simulated using a $6 \times 2\sqrt{3}$ unit cell, with a (3 × 5 × 1) Monkhorst–Pack mesh for the Brillouin zone integration. For the zigzag structure, we have used a unit cell with $b_1 = 23.15$ Å, $b_2 = 13.37$ Å lattice vectors. Due to the size of the system we have used the gamma point for the Brillouin zone integration. For the same reason, we also modeled the slab by only three layers of copper with the topmost layer relaxed.

We have simulated STM topographic images of the structures within the Tersoff and Hamman theory^{33,34} using the method described by Bocquet et al.³⁵

ASSOCIATED CONTENT

S Supporting Information

Experimental study of the adsorption of FeCp₂ on Cu(100). This material is available free of charge via the Internet at <http://pubs.acs.org/>.

AUTHOR INFORMATION

Corresponding Author

*E-mail: maider.ormaza@ipcms.unistra.fr

Notes

The authors declare no competing financial interest.

ACKNOWLEDGMENTS

This work has been supported by the Agence Nationale de la Recherche (Grant No. ANR-13-BS10-0016). L.L. acknowledges also financial support from the Agence Nationale de la Recherche through projects LabEx NIE and LabEx CSC. R.R. and N.L. acknowledge financial support from Spanish MINECO (Grant No. MAT2012-38318-C03-02 with joint financing by FEDER Funds from the European Union). P.A. acknowledges financial support from CONICET. ICN2 acknowledges support from the Severo Ochoa Program (MINECO, Grant SEV-2013-0295).

REFERENCES

- (1) Xiong, Z. H.; Wu, D.; Vardeny, Z. V.; Shi, J. Giant Magnetoresistance in Organic Spin-Valves. *Nature* **2004**, 427, 821–824.
- (2) Zhou, L.; Yang, S.-W.; Ng, M.-F.; Sullivan, M. B.; Tan; Shen, L. One-Dimensional Iron-Cyclopentadienyl Sandwich Molecular Wire

- with Half Metallic, Negative Differential Resistance and High-Spin Filter Efficiency Properties. *J. Am. Chem. Soc.* **2008**, *130*, 4023–4027.
- (3) Wang, L.; Cai, Z.; Wang, J.; Lu, J.; Luo, G.; Lai, L.; Zhou, J.; Qin, R.; Gao, Z.; Yu, D.; et al. Novel One-Dimensional Organometallic Half Metals: Vanadium-Cyclopentadienyl, Vanadium-Cyclopentadienyl-Benzene, and Vanadium-Anthracene Wires. *Nano Lett.* **2008**, *8*, 3640–3644.
- (4) Liu, R.; Ke, S.-H.; Baranger, H. U.; Yang, W. Organometallic Spintronics: A Dicobaltocene Switch. *Nano Lett.* **2005**, *5*, 1959–1962.
- (5) García-Suárez, V. M.; Ferrer, J.; Lambert, C. J. Tuning the Electrical Conductivity of Nanotube-Encapsulated Metallocene Wires. *Phys. Rev. Lett.* **2006**, *96*, 106804.
- (6) Shen, X.; Yi, Z.; Shen, Z.; Zhao, X.; Wu, J.; Hou, S.; Sanvito, S. The Spin Filter Effect of Iron-Cyclopentadienyl Multidecker Clusters: the Role of the Electrode Band Structure and the Coupling Strength. *Nanotechnology* **2009**, *20*, 385401.
- (7) Yang, J.-F.; Zhou, L.; Han, Q.; Wang, X.-F. Bias-Controlled Giant Magnetoresistance through CyclopentadienylIron Multidecker Molecules. *J. Phys. Chem. C* **2012**, *116*, 19996–20001.
- (8) Liu, R.; Ke, S.-H.; Yang, W.; Baranger, H. U. Cobaltocene as a Spin Filter. *J. Chem. Phys.* **2007**, *127*, 141104.
- (9) Morari, C.; Rungger, I.; Rocha, A. R.; Sanvito, S.; Melinte, S.; Rignanese, G.-M. Electronic Transport Properties of 1,1-Ferrocene Dicarboxylic Acid Linked to Al(111) Electrodes. *ACS Nano* **2009**, *3*, 4137–4143.
- (10) Welipitiya, D.; Green, A.; Woods, J. P.; Dowben, P. A.; Robertson, B. W.; Byun, D.; Zhang, J. Ultraviolet and Electron Radiation Induced Fragmentation of Adsorbed Ferrocene. *J. Appl. Phys.* **1996**, *79*, 8730–8734.
- (11) Waldorfried, C.; Welipitiya, D.; Hutchings, C. W.; de Silva, H. S. V.; Gallup, G. A.; Dowben, P. A.; Pai, W. W.; Zhang, J.; Wendelken, J. F.; Boag, N. M. Preferential Bonding Orientations of Ferrocene on Surfaces. *J. Phys. Chem. B* **1997**, *101*, 9782–9789.
- (12) Woodbridge, C. M.; Pugmire, D. L.; Johnson, R. C.; Boag, N. M.; Langell, M. A. HREELS and XPS Studies of Ferrocene on Ag(100). *J. Phys. Chem. B* **2000**, *104*, 3085–3093.
- (13) Durston, P.; Palmer, R. Adsorption and Decomposition of Ferrocene on Graphite Studied by HREELS and STM. *Surf. Sci.* **1998**, *400*, 277–280.
- (14) Svensson, K.; Bedson, T.; Palmer, R. Dissociation and Desorption of Ferrocene on Graphite by Low Energy Electron Impact. *Surf. Sci.* **2000**, *451*, 250–254.
- (15) Dowben, P.; Waldorfried, C.; Komesu, T.; Welipitiya, D.; McAvoy, T.; Vesco, E. The Occupied and Unoccupied Electronic Structure of Adsorbed Ferrocene. *Chem. Phys. Lett.* **1998**, *283*, 44–50.
- (16) Braun, K.-F.; Iancu, V.; Pertaya, N.; Rieder, K.-H.; Hla, S.-W. Decompositional Incommensurate Growth of Ferrocene Molecules on a Au(111) Surface. *Phys. Rev. Lett.* **2006**, *96*, 246102.
- (17) Quardokus, R. C.; Wasio, N. A.; Forrest, R. P.; Lent, C. S.; Corcelli, S. A.; Christie, J. A.; Henderson, K. W.; Alex Kandel, S. Adsorption of Diferrocenylacetylene on Au(111) Studied by Scanning Tunneling Microscopy. *Phys. Chem. Chem. Phys.* **2013**, *15*, 6973–6981.
- (18) Wasio, N. A.; Quardokus, R. C.; Forrest, R. P.; Lent, C. S.; Corcelli, S. A.; Christie, J. A.; Henderson, K. W.; Alex Kandel, S. Self-Assembly of Hydrogen-Bonded Two-Dimensional Quasicrystals. *Nature* **2014**, *507*, 86–89.
- (19) Heinrich, B. W.; Limot, L.; Rastei, M. V.; Iacovita, C.; Bucher, J. P.; Djimbi, D. M.; Massobrio, C.; Boero, M. Dispersion and Localization of Electronic States at a Ferrocene/Cu(111) Interface. *Phys. Rev. Lett.* **2011**, *107*, 216801.
- (20) Zhong, D.; Wedekind, K.; Blömker, T.; Erker, G.; Fuchs, H.; Chi, L. Multilevel Supramolecular Architectures Self-Assembled on Metal Surfaces. *ACS Nano* **2010**, *4*, 1997–2002.
- (21) Néel, N.; Limot, L.; Kröger, J.; Berndt, R. Rotation of C_{60} in a Single-Molecule Contact. *Phys. Rev. B* **2008**, *77*, 125431.
- (22) Haaland, A.; Nilsson, J. E.; Olson, T.; Norin, T. The Determination of Barriers to Internal Rotation by Means of Electron Diffraction. Ferrocene and Ruthenocene. *Acta Chem. Scand.* **1968**, *22*, 2653–2670.
- (23) Mohammadi, N.; Ganeshan, A.; Chantler, C. T.; Wang, F. Differentiation of Ferrocene DSd and DSh Conformers Using IR Spectroscopy. *J. Organomet. Chem.* **2012**, *713*, 51–59.
- (24) Coriani, S.; Haaland, A.; Helgaker, T.; Jørgensen, P. The Equilibrium Structure of Ferrocene. *ChemPhysChem* **2006**, *7*, 245–249.
- (25) Dunitz, J. D.; Orgel, L. E.; Rich, A. The Crystal Structure of Ferrocene. *Acta Crystallogr.* **1956**, *9*, 373–375.
- (26) Horcas, I.; Fernández, R.; Gómez-Rodríguez, J. M.; Colchero, J.; Gómez-Herrero, J.; Baro, A. M. WSXM: a Software for Scanning Probe Microscopy and a Tool for Nanotechnology. *Rev. Sci. Instrum.* **2007**, *78*, 013705.
- (27) Kresse, G.; Furthmüller, J. Efficiency of Ab-Initio Total Energy Calculations for Metals and Semiconductors Using a Plane-Wave Basis Set. *Comput. Mater. Sci.* **1996**, *6*, 15–50.
- (28) Blöchl, P. E. Projector Augmented-Wave Method. *Phys. Rev. B* **1994**, *50*, 17953–17979.
- (29) Kresse, G.; Joubert, D. From Ultrasoft Pseudopotentials to the Projector Augmented-Wave Method. *Phys. Rev. B* **1999**, *59*, 1758–1775.
- (30) Perdew, J. P.; Burke, K.; Ernzerhof, M. Generalized Gradient Approximation Made Simple. *Phys. Rev. Lett.* **1996**, *77*, 3865–3868.
- (31) Grimme, S. Semiempirical GGA-Type Density Functional Constructed with a Long-Range Dispersion Correction. *J. Comput. Chem.* **2006**, *27*, 1787–1799.
- (32) Tang, W.; Sanville, E.; Henkelman, G. A Grid-Based Bader Analysis Algorithm Without Lattice Bias. *J. Phys.: Condens. Matter* **2009**, *21*, 084204.
- (33) Tersoff, J.; Hamann, D. R. Theory and Application for the Scanning Tunneling Microscope. *Phys. Rev. Lett.* **1983**, *50*, 1998–2001.
- (34) Tersoff, J.; Hamann, D. R. Theory of the Scanning Tunneling Microscope. *Phys. Rev. B* **1985**, *31*, 805–813.
- (35) Bocquet, M.-L.; Lesnard, H.; Monturet, S.; Lorente, N. *Computational Methods in Catalysis and Materials Science*; Wiley-VCH: Weinheim, Germany, 2009.